Strojniški vestnik - Journal of Mechanical Engineering 52(2006)9, 558-567
UDK - UDC 669.13:620.178.3
Izvirni znanstveni članek - Original scientific paper (1.01)

# Trdnost litega železa in normaliziranega litega železa pri izmenični obremenitvi

## The Strength of as Cast Iron and Normalized Cast Iron Subjected to Cyclic Loading

Mindaugas Leonavičius[1] – Algimantas Krenevičius[1] – Stanislav Stupak[1] – Gediminas Petraitis[1] – Marijonas Šukšta[1] – Žilvinas Bazaras[2]
([1]Vilnius Gediminas Technical University, Lithuania; [2]Kaunas Univ. of Technology, Lithuania)

*V prispevku so predstavljeni rezultati eksperimentalnih in analitičnih raziskav pogosto se ponavljajoče utrujenosti posebnega litega in normaliziranega železa, ki ju kasneje v besedilu imenujemo GI (stopenjsko železo) in SGI (krogelno grafitno železo). Uveljavljeni vrsti železa smo spremenili, da bi dosegli boljše mehanske lastnosti in izboljšali odpornost proti nastajanju razpok, prav tako pa tudi njihovemu širjenju. Iz določenih mehanskih lastnosti vidimo, da normaliziranje spremeni mikrosestavo, poveča plastičnost in izenači meje prožnosti in trdnosti. V mikrosestavi opazovanega litega železa je vključen tudi grafit različnih velikosti, ki po toplotni obdelavi, pridobi krogelno obliko, poenoteno in manjšo velikost, tako da celotna mikrosestava postane bolj drobna. Po preizkušanju "kompaktne" izsredne napetosti CT (ASTM) na vzorcih smo za diagrame utrujenosti oblikovali območje faktorja razmerja rasti razpoke glede na jakost napetosti. In sicer za: GI lito železo $\Delta K_{th}$ = 6,5 do 8,6 MPa $\sqrt{m}$ ; za GI normalizirano lito železo $\Delta K_{th}$ = 8,2 do 10,3 MPa $\sqrt{m}$ ; zaSGI lito železoi $\Delta K_{th}$ = 8,0 do 9,6 MPa $\sqrt{m}$ in za SGI normalizirano lito železo $\Delta K_{th}$ = 8,7 do 9,8 MPa $\sqrt{m}$ . Pri mejnih vrednostih faktorjev jakosti napetosti smo ugotovili opazne razlike ter jih povezali z nepravilnostmi v sestavi na različnih straneh vzorcev, ki so nastale med izdelavo in postopkom normalizacije. Opazovali smo tudi vpliv $\Delta K_{th}$ na velikost razpok vzorcev litega in normaliziranega litega železa. Nadaljnje raziskave in analiza razpok so pokazale vpliv premajhne enotnosti sestave. Predlagan analitični izraz za $\Delta K_{th}$ in odvisnost mehanskih lastnosti lahko uporabimo za izračun trdnosti izmenično obremenjenih velikih kosov.*

**(Ključne besede: lito železo, utrujanje materialov, lom materialov, razpoke)**

*This paper presents the results of an experimental and analytical investigation of the high-cycle fatigue of special as-cast and normalized irons, which later in the text are referred to as GI (grade iron) and SGI (spherical graphite iron). Well-known types of cast iron have been modified to achieve better mechanical properties and an improved resistance to crack formation and development as well as propagation. The defined values of the mechanical properties show that the normalizing changes the microstructure, enlarges the plasticity and makes uniform the limits of yield and strength. The microstructures of the investigated as-cast irons include graphite of different sizes, which, after the heat treatment, acquire a spherical shape, unify and reduce in size, and the whole microstructure becomes finer. After testing the compact eccentric tension CT (ASTM) specimens, the crack-growth rate versus the stress intensity factor range for the fatigue diagrams were constructed, and the threshold stress intensity ranges were determined: for GI as cast iron $\Delta K_{th}$ = 6.5 to 8.6 MPa $\sqrt{m}$ ; for GI normalized cast iron $\Delta K_{th}$ = 8.2 to 10.3 MPa $\sqrt{m}$ ; for SGI as cast iron $\Delta K_{th}$ = 8.0 to 9.6 MPa $\sqrt{m}$ , and for SGI normalized cast iron $\Delta K_{th}$ = 8.7 to 9.8 MPa $\sqrt{m}$ . The significant differences in the threshold stress intensity factors were determined and related to the structural imperfections at the different sites of specimens formed during the manufacturing and normalization process. For specimens of as-cast and normalized cast iron, the dependence of $\Delta K_{th}$ on the crack size was observed. An additional investigation and the fracture analysis show that it was influenced by the absence of structural uniformity. The suggested analytical expression of the $\Delta K_{th}$ and the dependence of the mechanical properties can be applied for calculating the strength of cyclically loaded large-sized parts.*

**(Keywords: cast iron, fatigue, fracture, threshold, cracks)**

## 0 INTRODUCTION

The increase in the durability and reliability of machines, equipment and microstructures is connected with a rational application of mechanical properties, employing them to their limit values and with a large databank of values concerning deformation, strength and resistance to crack propagation. If the material of the element is uniform, it is sufficient to know the mechanical properties and values of the resistance to crack propagation and especially the threshold stress intensity range $\Delta K_{th}$, which can be applied in design calculations ([1] to [14]).

Details of large-size mining-industry equipment, which exceeds 5 m in size, are produced for a particular purpose from cast iron. The longevity of such details exceeds 25 years, and the number of loading cycles enters the gigacyclic range ($N > 10^8$ cycles). The casting of hull details from GI (grade iron) and gears from SGI (spherical graphite iron) and the following heat treatment is connected with some problems. To achieve the required microstructure, it necessary to apply a heat-treatment normalization, which is to guarantee a microstructural change throughout the whole of the large volume. During the normalization process it is necessary to obtain microstructures with a pearlite matrix, but usually there remains some part of ferrite, which is mild and undesirable. A ferrite matrix around graphite nodules has a negative influence on the mechanical properties: it reduces the hardness and the strength. In addition, it is more difficult to control the cooling rate of large-size products. In this case the desirable microstructure is obtained by means of special additives, e.g., Mg, Ca, Ce, Y, Nd, Pr [10], which are introduced to the metal when casting it. In order to adjust the different kinds of cast iron to particular production conditions, different technological processes are applied. The available technological means do not ensure the structural change at every point of the body. Therefore, it is necessary to know the microstructure, the mechanical properties and the resistance to crack propagation after casting and heat treatment. Having defined the indices of the resistance to crack propagation, it is possible to choose such safety coefficients that can guarantee the application of a non-uniform material for the production of important details ([1] to [5]). The pearlite matrix, being harder and stronger than the ferrite matrix, raises the mechanical properties, e.g., the fatigue strength. Spherical, fine-sized graphite remises the stress concentrations and increases the threshold stress-intensity factor.

In [5] and [6] an attempt was made to find the relationship between the threshold $\Delta K_{th}$, the yield limit $R_{p0.2}$, the strength limit $R_m$, *the* durability limit $\sigma_R$ and others. The threshold $\Delta K_{th}$ also depends on the stress ratio, the temperature, the environmental impact, the overloading, the structural peculiarities of the environment and other factors. However, there is a lack of data concerning the $\Delta K_{th}$ dependence on the mechanical properties and microstructure that may be changed in the process of heat treatment.

## 1 EXPERIMENT

For the experiment four as cast iron and four normalized cast-iron plates of both kinds (GI and SGI) were prepared. The chemical compositions of the investigated irons are presented in Table 1.

The chemical compositions, the setting and the casting procedures were produced at the foundry, and differ from well known similar cast irons used in the USA, Germany and Australia [10]. During heat treatment the investigated plates were settled at the various sites of the furnace beside large sized details. The microstructure of the GI as cast iron is shown in Figure 1a. The graphite is present in the shape of flakes of different size; the structural matrix is represented by ferrite-pearlite. At some points the spherical graphite was formed. The microstructure of the normalized GI as cast iron is shown in Figure 1a. The microstructure is fine-grained, the graphite is spherical, and the base of the microstructure shows pearlite with a small amount of ferrite.

The microstructure of the SGI as cast iron is shown in Figure 2a. It consists of flakes of different size and spherical graphite. The matrix is pearlite with irregularly situated ferrite, although sometimes bainite occurs. The microstructure after normalizing

Table 1. *Chemical composition*

| ***Cast iron*** | ***C*** | ***Si*** | ***Mn*** | ***Ni*** | ***Mo*** | ***Cu*** | ***Cr*** |
|---|---|---|---|---|---|---|---|
| | *[%]* | | | | | | |
| *GI* | *3.64* | *1.75* | *0.87* | *0.497* | *0.52* | *0.518* | *0.062* |
| *SGI* | *4.96* | *1.17* | *0.083* | *0.68* | *0.19* | *1.01* | – |

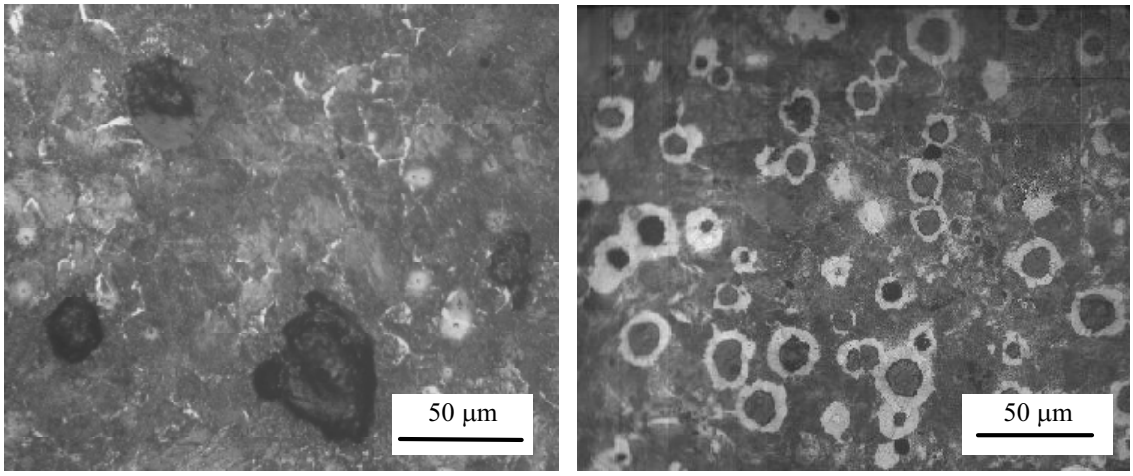


a b

Fig. 1. *Microstructure of GI iron: a – as cast, b – normalized*

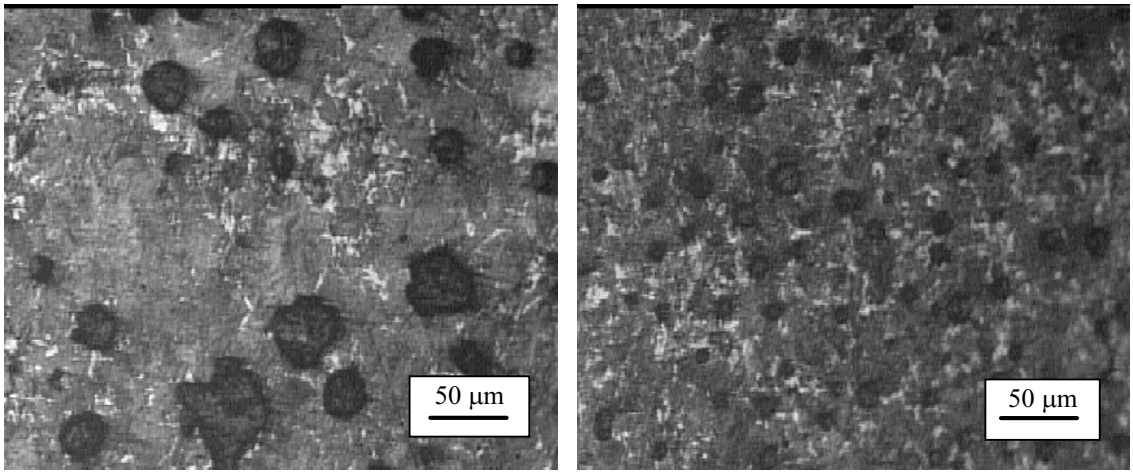


a b

Fig. 2. *Microstructure of SGI iron: a – as cast, b – normalized*

is shown in Figure 2b. It consists of spherical graphite, small-grained pearlite, bainite and ferrite. As we can see, normalizing makes the microstructure uniform and finer. The obtained nodular graphite is of a similar size (GI and SGI).

From all the plates, compact-tension specimens (CT) were fabricated. The values of the mechanical properties were defined; they are presented in Table 2. The hardness of the GI as cast iron is 250 to 277 BHN, the normalized is 228 to 256 BHN, and the hardness of the SGI as cast iron is 289 to 311 BHN, and the normalized one is 290 to 311 BHN. As we can see, in the process of heat treatment, the hardness changes slightly. The heat treatment process consists of normalization and annealing, in accordance with the real construction technological process circumstances.

For determining the threshold stress intensity factor range $\Delta K_{th}$, from GI and SGI cast irons, compact tension CT specimens were cut and shown in Figure 3.

After cyclic testing, additional cylindrical specimens (see Fig. 3) were cut from the CT specimens. The determined mechanical properties of each CT specimen were used to obtain the dependence between the threshold and the yield and the ultimate strength ratio ($R_m/R_{p0.2}$). In accordance with the ASTM E 647-00 methods [7], eight specimens of as cast iron, eight specimens of normalized GI cast iron and four as cast and four normalised SGI cast

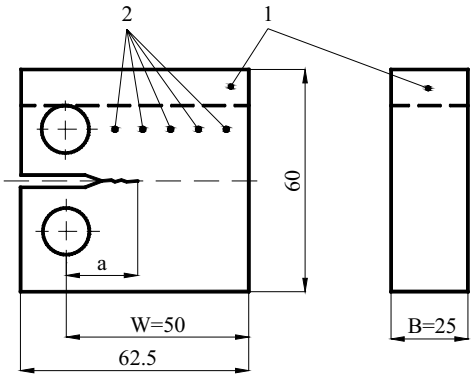


Fig. 3. *The CT specimen: 1 – tensile specimens preparation site; 2 – hardness measuring site*

Table 2. *Mechanical properties*

| ***Cast iron*** | | ***Yield strength*** | ***Ultimate tensile strength*** | ***Elongation*** |
|---|---|---|---|---|
| | | $R_{p0.2}$ *[MPa]* | $R_m$ *[MPa]* | *A [%]* |
| *GI* | *As cast* | *443 to 503* | *622 to 671* | *1.80 to 2.43* |
| | *Normalized* | *454 to 467* | *684 to 727* | *6.13 to 10.3* |
| *SGI* | *As cast* | *630 to 634* | *863 to 933* | *3.70 to 6.70* |
| | *Normalized* | *607 to 621* | *862 to 882* | *3.60 to 4.00* |

iron specimens were tested (frequency 30 Hz, stress ratio $r \approx 0$). By applying the methods of calculation ([7] and [8]), the crack growth rate versus stress intensity factor range diagrams for fatigue were compiled and the stress intensity factor range $\Delta K$ (the variation of the stress intensity factor in a loading cycle) defined; this value was calculated using the formula:

$$\Delta K = \frac{\Delta F}{B \cdot W^{1/2}} f(\lambda) \qquad (1),$$

where $\Delta F$ is the force range (the difference between the maximum and the minimum forces in a loading cycle), $B$ is the thickness of the specimen (see Fig. 3.), $W$ is the width of the specimen, $f(\lambda)$ is the geometric factor, calculated using the following :

$$f(\lambda) = \frac{(2+\lambda)}{(1-\lambda)^{3/2}}\left(0.886 + 4.64\lambda - 13.32\lambda^2 + 14.72\lambda^3 - 5.6\lambda^4\right) \qquad (2),$$

where $\lambda = a/W$, and $a$ is the crack size.

The crack growth rate versus stress intensity factor range fatigue diagram of specimens of GI as cast iron is shown in Figure 4a. The crack growth rate versus stress-intensity factor range fatigue diagram of the normalized cast iron is presented in Figure 4b. The threshold $\Delta K_{th}$ = 6.5 to 8.6 MPa$\sqrt{\text{m}}$, and for the normalized cast iron $\Delta K_{th}$ = 8.2 to 10.3 MPa$\sqrt{\text{m}}$. The presented data show that normalisation increases the resistance to crack initiation and propagation, i.e., it increases the threshold stress-intensity range.

The crack growth rate versus stress intensity factor range fatigue diagram of specimens of SGI as cast iron is presented in Figure 5a and the normalized cast iron is presented in Figure 5b. The threshold for as cast iron $\Delta K_{th}$ = 8.0 to 9.6 MPa$\sqrt{\text{m}}$, and for normalized cast iron $\Delta K_{th}$ = 8.7 to 9.8 MPa$\sqrt{\text{m}}$.

In references [3], [5], [8] and [12] the dependence of $K_c$ (fracture toughness) on crack size, crack arrest conditions and the relationship of these on other various factors is discussed. From our investigation it is possible to see that in some specimens, under a different crack size, different thresholds appear: when the depth of the fatigue crack increases, the threshold stress intensity range increases, too. In order to explain this phenomenon and to check whether some accidental factors have influenced the results, an additional SGI normalized cast iron compact specimen was tested. The produced crack growth rate versus stress intensity factor range diagram is shown in Figure 6. We can see in it that different $\Delta K_{th}$ values correspond to different crack sizes (16.2, 18.5, 21.1, 25.2 and 29.8 mm). Some difference can be explained by the crack front in the stress state in the crack tip; the crack front results from an inhomogeneous microstructure after the heat treat-

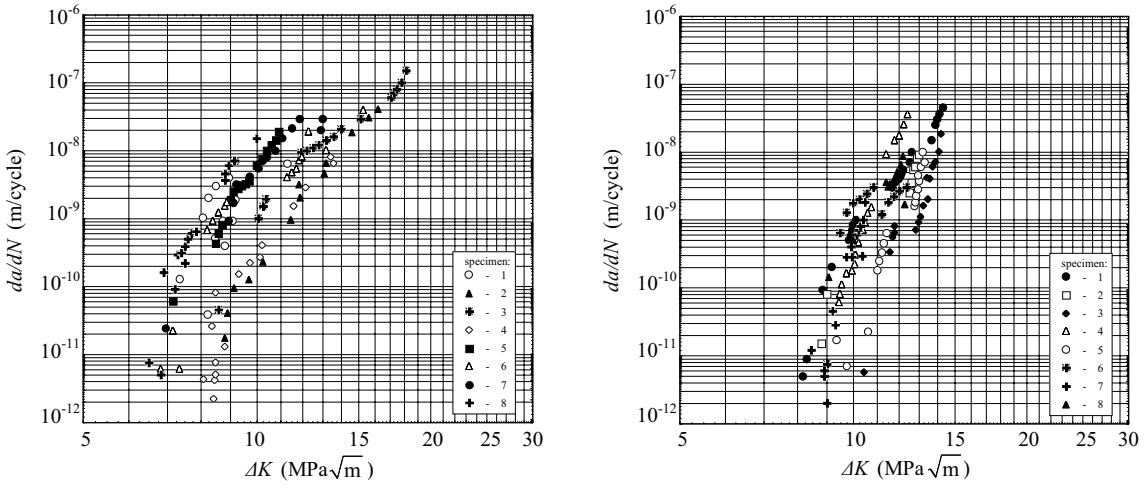


Fig. 4. *Crack growth rate versus stress-intensity factor range of GI iron: a – as cast iron, b – normalized iron*

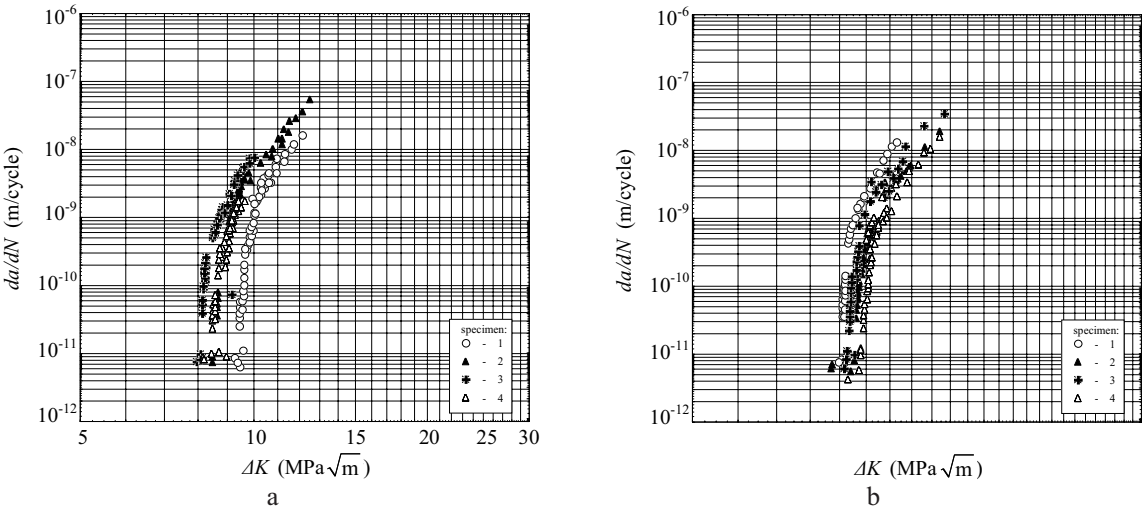


Fig. 5. *Crack growth rate versus stress-intensity factor range of SGI iron: a – as cast, b – normalized*

ment and, consequently, the fracture mechanism changes.

The fracture of an additional CT sample is shown in Fig 7. The observed crack stopping lines (defined 1 to 4) developed because of the change of load during the crack propagation rates decreasing procedures. At these lines the thresholds were determined: 1 - $\Delta K_{th} = 8.72\ \text{MPa}\sqrt{\text{m}}$ ($2.816 \cdot 10^6$ cycles), 2 - $\Delta K_{th} = 8.75\ \text{MPa}\sqrt{\text{m}}$ ($7.8495 \cdot 10^6$ cycles), 3 - $\Delta K_{th} = 9.41\ \text{MPa}\sqrt{\text{m}}$ ($13.718 \cdot 10^6$ cycles), and 4 - $\Delta K_{th} = 9.81\ \text{MPa}\sqrt{\text{m}}$ ($21.186 \cdot 10^6$ cycles). The surface of the crack development and the fatigue enlarging is shown in Fig 8a. The crack structure is reminiscent of a fragile disintegration, which usually takes place when the intergranular ties, for some reasons (a contaminated intergranular laminar, the presence of secondary phases, the segregation of alloying additives, etc.), are weaker than structural grains. At the top of the groove there are many crack focuses (up to 1 mm length), which at a different depth have united to form a main crack. Fig 8b shows the middle part of the fatigue-crack propagation area. Spaces that are close to crack stopping lines (defined 1 and 2) are of different roughness. The furrows and the different crack stopping lines show an irregular cracking front development and some inhomogeneity of the microstructure. The CT specimen's static fracture surface is depicted in Fig 8c. The fracture surface shows the

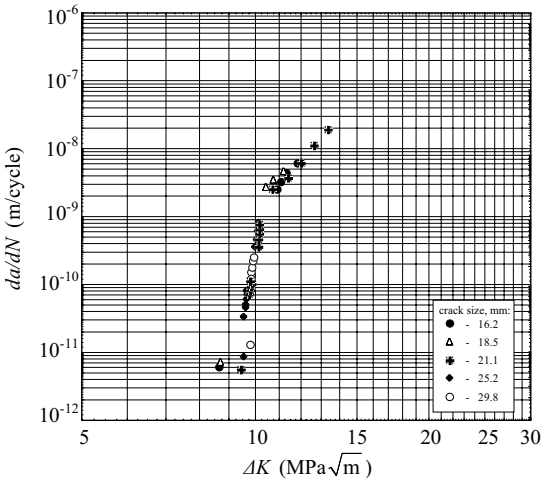


Fig. 6. *Crack growth rate versus stress intensity factor range of additional testings*

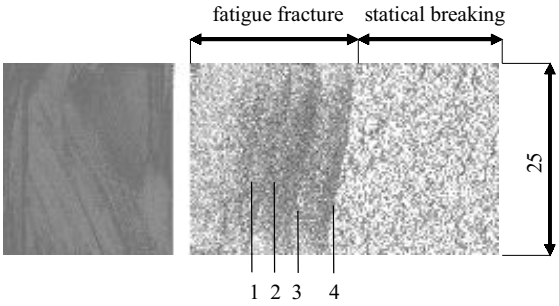


Fig. 7. *Fracture of CT specimen: 1 to 4 are crack-stopping tracks*

character of a fragile disintegration. In the fracture small pits can be seen; they have developed in the place of cavities, and around them crests have developed in the place of the connections. The cavities develop out of micro-pores, micro-cavities and micro-fissures in the material or arise under the influence of strains. At their base inhomogeneous formations can be found. It was observed that fragile streaks develop in the pearlite and in the plastic zones in the ferrite.

During fatigue precracking and the crack propagation rate decreasing procedure, the disintegration character changes. By decreasing the crack propagation rates to $da/dN$=$10^{-12}$ m/cycle the threshold stress intensity factor $\Delta K_{th}$ rises; however, the disintegration process becomes unclear in terms of its relation to the microstructure [5].

## 2 ANALYSIS OF THE MECHANICAL PROPERTIES AND THE THRESHOLD

In fracture mechanics, the general expression for the stress intensity factor is ([3], [5] and [8]):

$$K_I = Y \cdot \sigma \sqrt{a + a_0} \qquad (3),$$

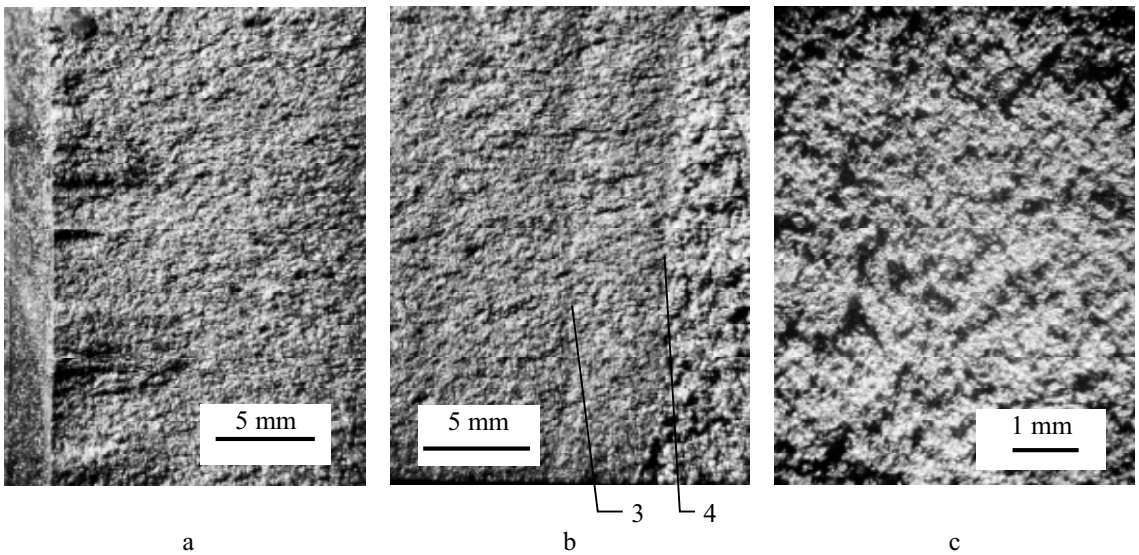


Fig. 8. *Fracture surface: a – fatigue crack initiation area, b – middle part of the fatigue crack propagation area (3 - $\Delta K_{th}$ = 9.41 MPa$\sqrt{m}$, N = 13.178 · $10^6$ cycles, 4 - $\Delta K_{th}$ = 9.81 MPa$\sqrt{m}$, N = 21.186 · $10^6$ cycles), c – static fracture surface*

where $Y$ is geometric factor; $\sigma$ is the stress, $a$ is the crack size, $a_0$ is the structural defect size.

When $a = 0$, $\sigma = \sigma_R$ (durability limit), $K_I = \Delta K_{th}$, we have the threshold stress intensity range:

$$\Delta K_{th} = Y \cdot \sigma_R \sqrt{a_0} \qquad (4).$$

The resistance to crack initiation and propagation depends on many factors and predetermines the longevity of the structural element: it depends directly on microstructure formations (inclusions, cavities, slide belts, defects of production and the exploitation). According to the experimental data obtained, the relations were set between the threshold $\Delta K_{th0}$ (when stress ratio $r \approx 0$) and the mechanical property values ratio $R_m/R_{p\,0.2}$, presented in Fig 9. A linear dependence is described by such a function:

$$\Delta K_{th0} = 5.087 \frac{R_m}{R_{p0.2}} + 1.306 \qquad (5).$$

The obtained correlation coefficient equals 0.62. The results of a calculation using Formula (5) are compared with those obtained by experiments, and are presented in Table 3. The experimental values $\Delta K_{th,exp}$ were determined from the crack growth rate versus stress intensity factor range fatigue diagrams. In accordance with the ASTM the threshold stress-intensity factors are determined when the fatigue crack propagation rates are at $10^{-10}$ m/cycle. However, for the reassurance of longevity of mineral mining equipment the threshold stress-intensity factors must be taken from $10^{-10}$ to $10^{-12}$ m/cycle. The calculated values $\Delta K_{th,cal.}$ were determined from Equation (5). The additional points in Table 3 characterize the scatter of the threshold $\Delta K_{th}$ values. We can see that for the as-cast GI and SGI irons there are bigger deflections from the obtained dependence.

The limit stress intensity factor $\Delta K_{th}$ also depends on the asymmetry, the temperature, the environmental effect, the overloading, the inhomogeneity and other factors. The investigations [3], [5], [6] and [8] report an increase of the threshold $\Delta K_{th}$ and the fatigue crack growth rate with a change of stress ratio from 0 to 0.9. Under conditions of larger stress ratios ($r > 0.6$ to 0.7), the fracture process changes: its mechanism starts approaching that of the static fracture. Because the crack during the loading process remains open all the time, the threshold $\Delta K_{th}$ and the fatigue crack growth rate in a uniform stress intensity factor range becomes more independent of asymmetry. When the stress change is negligible ($r > 0.9$), the cyclic fracture becomes closer to a static fracture.

The shape of the fatigue diagram deforms and, having achieved higher tension values, abruptly breaks. Under conditions of a negative symmetry, its impact on the threshold stress intensity range $\Delta K_{th}$ considerably decreases; it is influenced by crack closing. Under conditions of a negative cycle asymmetry, the compressive stresses are often neglected, considering that $K_{min} = 0$ and $\Delta K = K_{max}$.

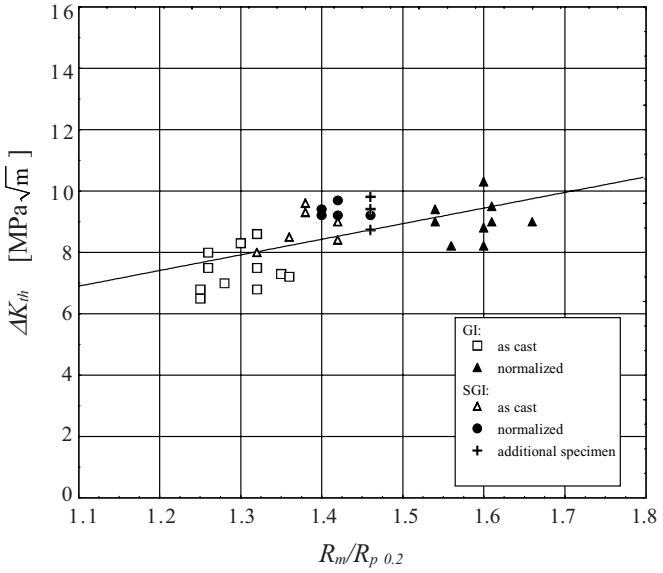


Fig. 9. *Dependence between* $\Delta K_{th}$ *and* $R_m/R_{p\,0.2}$

Table 3. *Comparison of experimental and calculated values*

| **Cast iron** | | **Specimen** | $R_m/R_{p\,0.2}$ | $\Delta K_{th,\,exp}$ | $\Delta K_{th,\,cal}$ | **Difference** |
|---|---|---|---|---|---|---|
| | | | | $[MPa\sqrt{m}]$ | $[MPa\sqrt{m}]$ | [%] |
| GI | As cast | 1 | 1.30 | 8.3 | 7.9 | 4.6 |
| | | 2 | 1.35 | 7.3 | 8.2 | 12.0 |
| | | 3 | 1.32 | 8.6 | 8.0 | 6.7 |
| | | 4 | 1.26 | 7.5 | 7.7 | 2.3 |
| | | 5 | 1.36 | 7.2 | 8.2 | 14.2 |
| | | 6 | 1.32 | 6.8 | 8.0 | 18.0 |
| | | 7 | 1.28 | 7.0 | 7.8 | 11.7 |
| | | 8 | 1.25 | 6.5 | 7.7 | 17.9 |
| | Normalized | 1 | 1.56 | 8.2 | 9.2 | 12.7 |
| | | 2 | 1.60 | 8.8 | 9.4 | 7.3 |
| | | 3 | 1.60 | 10.3 | 9.4 | 8.3 |
| | | 4 | 1.54 | 9.4 | 9.1 | 2.8 |
| | | 5 | 1.61 | 9.5 | 9.5 | 0 |
| | | 6 | 1.66 | 9.0 | 9.8 | 8.3 |
| | | 7 | 1.60 | 8.2 | 9.4 | 15.2 |
| | | 8 | 1.54 | 9.0 | 9.1 | 1.6 |
| SGI | As cast | 1 | 1.38 | 9.3 | 8.3 | 10.5 |
| | | 2 | 1.32 | 8.0 | 8.0 | 0.26 |
| | | 3 | 1.36 | 8.5 | 8.2 | 3.2 |
| | | 4 | 1.42 | 9.0 | 8.5 | 5.2 |
| | Normalized | 1 | 1.40 | 9.4 | 8.4 | 10.3 |
| | | 2 | 1.46 | 9.2 | 8.7 | 5.1 |
| | | 3 | 1.40 | 9.2 | 8.4 | 8.4 |
| | | 4 | 1.42 | 9.7 | 8.5 | 12.1 |
| SGI additional specimen | Normalized | 1 | 1.46 | 8.7 | 8.7 | 0 |
| | | | | 8.75 | | 0.19 |
| | | | | 9.4 | | 7.2 |
| | | | | 9.8 | | 11.0 |
| Additional point GI | As cast | 4 | 1.26 | 8.0 | 7.7 | 3.6 |
| | | 6 | 1.32 | 7.5 | 8.0 | 6.9 |
| | | 8 | 1.25 | 6.8 | 7.7 | 12.7 |
| | Normalized | 5 | 1.61 | 9.0 | 9.5 | 5.5 |
| Additional point SGI | As cast | 1 | 1.38 | 9.6 | 8.3 | 13.3 |
| | | 4 | 1.42 | 8.4 | 8.5 | 1.5 |
| | Normalized | 4 | 1.42 | 9.2 | 8.5 | 7.3 |

In practice, crack growth rate versus stress intensity factor range diagrams are most often applied with comparatively small stress range values ($r$ = 0.05 to 0.1), because a larger cycle asymmetry may distort the kinetics of crack propagation. When calculating the negative stress ratio, it is difficult in laboratories to realise the negative part of the loading cycle. The stress ratio changes under service conditions in rather large ranges and influences the crack propagation. When calculating real structures, it is necessary to make corrections in the stress states, in the dimensions, the stress concentration and the surface conditions ([12] to [14]). For a practical calculations of $\Delta K_{th}$, when assessing the stress ratio $r$ [6]:

$$\Delta K_{th} = \Delta K_{th0}(1 - r)^{\gamma} \quad (6),$$

where $\Delta K_{th0}$ is the limit interval of the stress intensity factor, when $r$ = 0; $\gamma$ is a coefficient dependent on the material and fluctuates from 0.5 up to 1. Formula (6) shows a good agreement for steel when $0 < r < 0.6$.

Considering the experimental data and the performed analysis it is possible to get equations that are suitable for constructional elements and investigated cast irons. By using Formulae (5) and (6), it is possible to write:

$$\Delta K_{th} = \left(5.087\frac{R_m}{R_{p0.2}} + 1.306\right)(1 - r)^{\gamma} \quad (7).$$

If there is a crack of length 2*l* on the surface of a detail, the crack development will be stopped when the limit stress interval correspondent $\Delta K_{th}$ does not exceed $\Delta\sigma_{th}$ calculated with Formula (4):

$$\Delta\sigma_{th} = \frac{\Delta K_{th}}{Y\sqrt{2l}} \qquad (8).$$

By rearranging Formula (8) we obtain the stress range that is in accordance with the threshold stress intensity factor range $\Delta K_{th}$:

$$\Delta\sigma_{th} = \frac{\left(5.087\frac{R_m}{R_{p0.2}} + 1.306\right)(1-r)^{\gamma}}{Y\sqrt{2l}} \qquad (9).$$

The expression obtained can be used for calculating the strength of cyclically loaded large-size details, which remain inhomogeneous after the casting and heat treatment processes. To validate Equation (9) for details from the cast iron with another stress ratio an additional analysis based on experiments is necessary. However, it must be mentioned that the dependence between the threshold and the hardness of the specimens was not observed.

## 3 CONCLUSIONS

After performing an experimental analysis of the investigations and the results of as cast and normalized cast iron we found the following:

1. Normalizing of the details of large-size details makes the material structure uniform and improves the values of the mechanical properties and the resistance to fatigue-crack formation and propagation, although the variation in the identified properties is large. The identified threshold stress intensity range of the GI as-cast is $\Delta K_{th}$ = 6.5 to 8.6 MPa$\sqrt{\text{m}}$ ; and for normalized cast iron, $\Delta K_{th}$ = 8.2 to 10.3 MPa$\sqrt{\text{m}}$ . The threshold for SGI as cast is $\Delta K_{th}$ = 8.0 to 9.6 MPa$\sqrt{\text{m}}$ ; and for normalized cast iron, $\Delta K_{th}$ = 8.7 to 9.8 MPa$\sqrt{\text{m}}$ .
2. The crack growth rate versus stress intensity factor range diagrams created for as cast and normalized cast iron show when the crack growth *da/dN* = $10^{-12}$ m/cycle threshold stress intensity range depends on the crack depth. The threshold $\Delta K_{th}$ increases when the crack depth increases.
3. The established expression between the threshold stress intensity range $\Delta K_{th}$ and the ultimate and the yield strength ratio $R_m/R_{p0.2}$ can be applied for a design strength calculation of the cyclically loaded structural elements with an inhomogeneous state complex. The identified function describes satisfactorily (the obtained correlation coefficient equals 0.62) the experimental data. For a wider application of the obtained dependence an additional analysis and calibration are required.

## 4 REFERENCES


[1] Marrow T.J., H. Cetinel, S. MacDonald, P.J. Withers, A. Venslovas, M. Leonavičius (2002) *Proceedings of the 14th Biennial Conference on Fracture – ECF14,* Vol. II / III, Sheffield, UK: EMAS, 2002, 443-450.

[2] Leonavičius, M., M. Šukšta, S. Stupak, G. Petraitis (2003) *Mechanika*, No 5(43), 13-18.

[3] Hertzberg R. W. (1996) Deformation and fracture mechanics of engineering materials. *John Willey & Sons Inc*., New York – Singapore.

[4] Dorazil E. (1991) High strength austempered ductile cast iron. *Ellis Horwood*, Prague.

[5] Панасюк В.В. (1990) Механика разрушения и прочность материалов. *Наукова думка*, Киев.

[6] Kocanda S. (1985) Zmêczeniowe pêkanie metali. *Wydawnictwo naukowo-techniczne*, Warszawa.

[7] ASTM E 647-00. (2000) Standard Test Method for Measurement of Fatigue Crack Growth Rates.

[8] Anderson T.L. (1991) Fracture mechanics. Fundamentals and Application, *CRC Press*, Boston.

[9] Foth S.C., J.C. Newman, R.G Forman (2003) *International Journal of Fatigue*, No 25, 9-15.

[10] Žvinys J. (1999) Konstrukciniai lydiniai. Ketus. *Technologija*, Kaunas.

[11] Ботвина Л.Р. (2004) *Заводская лаборатория. Диагностика материалов,* No 4, 41-51.

[12] Broek D. (1989) The practical uses of fracture mechanics. *Kluwer Academic Publishers*, Dordrech/ Boston/London.

[13] Hudak Jr.S.J. (1981) *Journal of Engineering Materials and Technology*, No 1, 28-39.

[14] Трощенко В.Т. (2000) *Проблемы прочности,* No 5, 34-43.

Authors' Address:
Prof.Dr. Habil. Mindaugas Leonavičius
Prof.Dr. Algimantas Krenevičius
Prof.Dr. Stanislav Stupak
Mag. Gediminas Petraitis
Prof.Dr. Marijonas Šukšta
Vilnius Gediminas Technical Univ.
Dept. Strength of Materials
Sauletekio str. 11, LT-10223
Vilnius - 40, Lithuania
minleo@fm.vtu.lt
ma@fm.vtu.lt
stupakas@adm.vtu.lt
gedp@fm.vtu.lt
marijonas.suksta@fm.vtu.lt

Prof. Dr. Žilvinas Bazaras
Kaunas Univ. of Technology
Dept. of Transport Engineering
Kestucio str. 27, LT-44025
Kaunas, Lithuania
zilvinas.bazaras@ktu.lt

Prejeto: 15.6.2005
Received:
Sprejeto: 22.6.2006
Accepted:
Odprto za diskusijo: 1 leto
Open for discussion: 1 year